# Decoupling technique of patch antenna arrays with shared substrate by suppressing near-field magnetic coupling using magnetic metamaterials*

Zhaotang Liu(柳兆堂)[1], Jiafu Wang(王甲富)[1,†], Shaobo Qu(屈绍波)[1,‡], Jieqiu Zhang(张介秋)[1], Hua Ma(马华)[1], Zhuo Xu(徐卓)[2], and Anxue Zhang(张安学)[3]

[1] *College of Science, Air Force Engineering University, Xi'an* 710051, *China*
[2] *Key Laboratory of Electronic Materials Research Laboratory of the Ministry of Education, Xi'an Jiaotong University, Xi'an* 710049, *China*
[3] *School of Electronics and Information, Xi'an Jiaotong University, Xi'an* 710049, *China*

(Received 7 May 2016; revised manuscript received 13 January 2017; published online 10 March 2017)

In this paper, we propose the decoupling technique of patch antenna array by suppressing near-field magnetic coupling (NFMC) using magnetic metamaterials. To this end, a highly-integrated magnetic metamaterials, the substrate-integrated split-ring resonator (SI-SRR), is firstly proposed to achieve negative permeability at the antenna operating frequency. By integrating SI-SRR in between two closely spaced antennas, magnetic fields are blocked in the shared substrate due to negative permeability of SI-SRR, reducing NFMC between the two antennas. To verify the technique, a prototype was fabricated and measured. The measured results demonstrated that the isolation can be enhanced by more than 17 dB even when the gap between the two patch antennas is only about 0.067$\lambda$. Due to high integration, this technique provides an effective alternative to high-isolation antenna array.

**Keywords:** antenna isolation, antenna array, near-field magnetic coupling, magnetic metamaterials, negative permeability

**PACS:** 73.20.Mf, 41.20.Jb, 78.20.Bh, 84.40.Ba **DOI:** 10.1088/1674-1056/26/4/047301

## 1. Introduction

Multiple input multiple output (MIMO) systems have been researched for many years since they can provide a significant increase in wireless channel capacity without the need for additional transmitting power or spectrum.[1,2] On the other hand, patch antennas are pervasively used in communication systems for the reason that they can provide high directivity, narrow beam, large aperture efficiency and a variety of radiation patterns. Most importantly, they can be conveniently conformed to curved objects. For these reasons, patch antennas are preferred in MIMO systems for commercial applications.[3]

High isolation among adjacent antenna elements is one of the key requirements in MIMO systems. In order to solve the conflict between compactness and isolation, researchers have done a lot of research work and many techniques for reducing the mutual couplings between antenna array have been proposed, typically including: (i) the electromagnetic band-gap (EBG) structure,[4,5] which forms a narrow stop-band for surface waves along the substrate surface into substrate between the space of adjacent antennas; (ii) electromagnetic isolation (EMI) walls, which are used along the radiating edges of a patch on a ground plane[6] to isolate fields above the substrate; (iii) polarization modulation of different antennas,[7] which make transmission antennas and received antennas with different polarization states; (iv) etching metallic patterns[8–10] between patch antennas to suppress surface waves; (v) double ground-plane side walls defected with a lattice pattern of slots to form a defected wall structure (DWS) that are erected vertically next to adjacent antennas.[11] Most of the above-mentioned techniques aim to suppress surface waves above the substrate. In fact, the mutual coupling between adjacent antennas in the substrate is much stronger since the fields in the substrate is confined in the narrow space between the patch and ground plane and the field intensity is greatly enhanced due to the low profile, especially the magnetic field component. Because of this, strong near-field magnetic coupling (NFMC) exists in the substrate for adjacent patch antennas. Therefore, it is significant for high isolation patch antenna array if NFMC in the substrate can be suppressed.

In this paper, we propose decoupling technique of patch antenna array by suppressing NFMC in substrate using magnetic metamaterials. To this end, a magnetic metamaterials unit cell (MMUC), which is a substrate-integrated split-ring

*Project supported in part by the National Natural Science Foundation of China (Grant Nos. 61331005, 61471388, 61501503, 61501502, 61501497, 51575524, 61302023, and 11304393) and the Natural Science Foundation of Shaanxi Province, China (Grant Nos. 2015JM6300 and 2015JM6277).

†Corresponding author. E-mail: wangjiafu1981@126.com
‡Corresponding author. E-mail: qushaobo@mail.xjtu.edu.cn

© 2017 Chinese Physical Society and IOP Publishing Ltd 

resonator (SI-SRR) is firstly designed. The MMUC responds strongly to magnetic fields and exhibit negative effective permeability in the resonance regime. By careful design, the resonant frequency of MMUC is made the same as the operating frequency of the patch antennas. Due to negative permeability, most of the near-field magnetic fields threading through the SI-SRR are bounced back and cannot penetrate into the substrate region of adjacent patch antenna. The center-to-center spacing between the two adjacent patch antennas we proposed is about $0.35\lambda$ and the gap between the two antenna patches is about $0.067\lambda$. Both the simulation and experiment show that this technique can enhance the isolation by about 17.1 dB. This method provides a new mechanism to suppress mutual coupling of antennas such as in MIMO systems, and it is suitable mostly to size and cost-limited MIMO applications that require high isolation.

## 2. Structure design and analysis

### 2.1. Magnetic metamaterials design and analysis

As we all know, magnetic metamaterials can achieve negative permeability in its resonance regime. Since the effective permeability is negative while the permittivity is still positive, the propagation constant of electromagnetic (EM) waves in magnetic metamaterials is purely imaginary, and hence EM waves cannot transmit through it. One of the most typical magnetic metamaterials is the split-ring resonator (SRR).[12] SRR is excited by the external magnetic fields and require magnetic fields lines to thread through the structure to obtain the negative permeability.[13] Large number of numerical simulations has been taken to study the properties of transmission spectra[14,15] of SRRs. We model the MMs as a dispersive anisotropic medium, which can be characterized by the permeability tensor $\bar{\bar{\mu}}$:[12]

$$\bar{\bar{\mu}} = \begin{bmatrix} 1 & 0 & 0 \\ 0 & \mu_y(\omega) & 0 \\ 0 & 0 & 1 \end{bmatrix},$$

where $\mu_y(\omega)$ follows a Lorentz model:

$$\mu_y(\omega)\mu_0 \frac{\omega_p^2}{\omega_0 - i\gamma\omega - \omega^2}, \tag{1}$$

in which $\omega_p = 14.55 \times 10^9$ rad·s$^{-1}$, $\omega_0 = 46 \times 10^9$ rad·s$^{-1}$, $\gamma = 1 \times 10^8$ rad·s$^{-1}$.

To conserve the low-profile property of the patch antenna array, the normal-incidence SRR must be used. There by, we designed the normal-incidence MMUC, as shown in Fig. 1(a). The MMUC is composed of a grounded FR-4 dielectric substrate ($\varepsilon_r = 4.3$, $\tan\delta = 0.025$) with two metalized vias connected metallic patterns on both of sides. One side of substrate is etched with copper patterns and the other side is covered fully with copper. Two metalized via holes with the radius $r = 0.4$ mm connect copper ground and the metallic pattern on the substrate. Geometrical sizes of the MMUC are: $w_1 = 3.0$ mm, $l_1 = 12.0$ mm, $t = 1.6$ mm, $w_2 = 2.5$ mm, $w_3 = 0.4$ mm, $l_2 = 4.6$ mm, $g = 0.4$ mm. Magnetic resonators are excited when external magnetic fields get though the loop of unit cell. The fundamental resonance mode is a magnetic resonator is the magnetic dipole mode. Typically, the resonance behavior of a magnetic dipole can be described by the Lorentz model,[15] and equation (2) can be written as:

$$\mu_y(\omega) = 1 - \frac{\omega_p^2}{\omega_0 + i\gamma\omega_m - \omega_m^2}, \tag{2}$$

where $\omega_m / \sqrt{(L_1 + L_2 + L_3)C}$ is the resonance frequency. We can adjust the dimensions of $l_2$, $w_2$, and $w_3$ to change the effective inductances and effective capacitance of structure and thus to tune the resonant frequency. Figure 1(b) presents the corresponding equivalent circuit of each part of the MMUC, where $C$ denotes the effective capacitance between the two parallel horizontal strips, $L_1$ the effective inductances of the metalized vias, and $L_2$ and $L_3$ the effective inductances of the metalized strips and cupreous back, respectively.

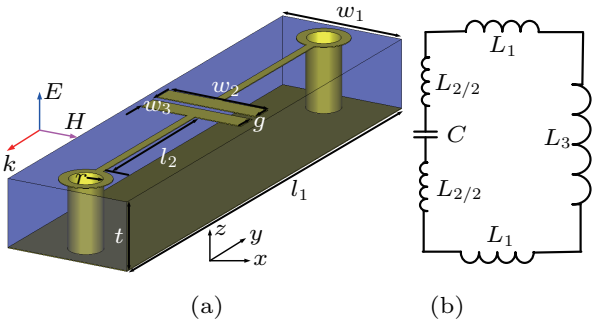



**Fig. 1.** (color online) The structure (a) and equivalent circuit (b) of the MMUC.

The simple and adjustable MMUC is simulated using the frequency-domain solver in CST Microwave Studio. The boundary conditions are set as such that in $\hat{x}$ and $\hat{z}$ directions are periodic boundaries, and in $\hat{y}$ direction is open boundary. To obtain the response of MMUC, EM wave is incident along $\hat{y}$ direction, with the magnetic field and electric filed in $\hat{x}$ and $\hat{z}$ direction, respectively. The simulated results are shown in Fig. 2. As shown in Fig. 2(a), there is a deep dip the transmission in the range of 3.9 GHz–4.1 GHz ($\leq -10$ dB) with $S_{11} = -1.5$ dB, $S_{21} = -16$ dB at the dip. In order to check the characteristic of the resonance, we retrieved the effective parameters, as shown in Fig. 2(b). The real part of effective permeability $\mu = -1.2$ at 4.0 GHz. In 3.8 GHz–4.25 GHz, the effective permeability is negative, which indicates strong magnetic resonance occurs in this regime.

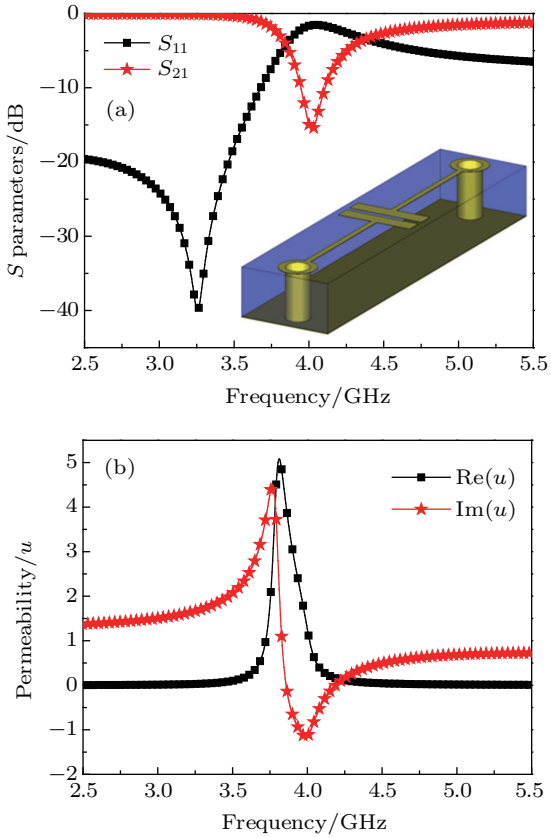



**Fig. 2.** (color online) The *S* parameters (a) and effective parameters (b) of the SI-SRR magnetic metamaterials.

### 2.2. Antenna array design and analysis

A two-element patch antenna array operating at 4.0 GHz is designed and the model of the antennas is shown in Fig. 3(a). Figure 3(b) gives the simulated results. The geometrical parameters of the patch antennas are: $a_1 = 51.0$ mm, $a_2 = 23.0$ mm, $b_1 = 40.0$ mm, $b_2 = 16.3$ mm, $b_3 = 16.75$ mm. The gap between the two patch antennas is 3.0 mm. Figure 3(b) shows the simulated *S* parameters when only one of the two antennas (antenna 1) is fed. It can be found that the magnitude of $S_{21}$ is up to −9.5 dB at the central operating frequency. The mutual coupling between the two patch antennas is very strong at 4.0 GHz, which is detrimental to normal operation of antennas especially in high-power uses.

To give an intuitive illustration of the strong in-substrate near-field coupling, the *H*-field vector distribution of the two closely packed patches on *xy* plane and *xz* plane at 4 GHz in the substrate are plotted in Figs. 4(a) and 4(b), respectively. It can be seen from Fig. 4(a) that the magnetic coupling is so strong that the magnetic field intensity for antenna 2 is nearly comparable to that for the fed antenna 1. For the patch antenna, according to the transmission line theory[16] and cavity model theory,[17] the antenna substrate can be regarded as a general transmission media. The magnetic field around the patch exists in both the substrate and air, forming a closed loop rounding the radiation patch. For patch antenna array with a shared substrate, the excited magnetic field of the active antenna will couple into the adjacent passive antennas to form the closed magnetic field loop through the substrate and air, which will result in intense NFMC in the substrate. As shown in Fig. 4(b), the *H*-field vector formed a closed loop and the near-field magnetic field is coupled into antenna 2 mostly through the shared substrate, resulting in intense NFMC between the two antennas.

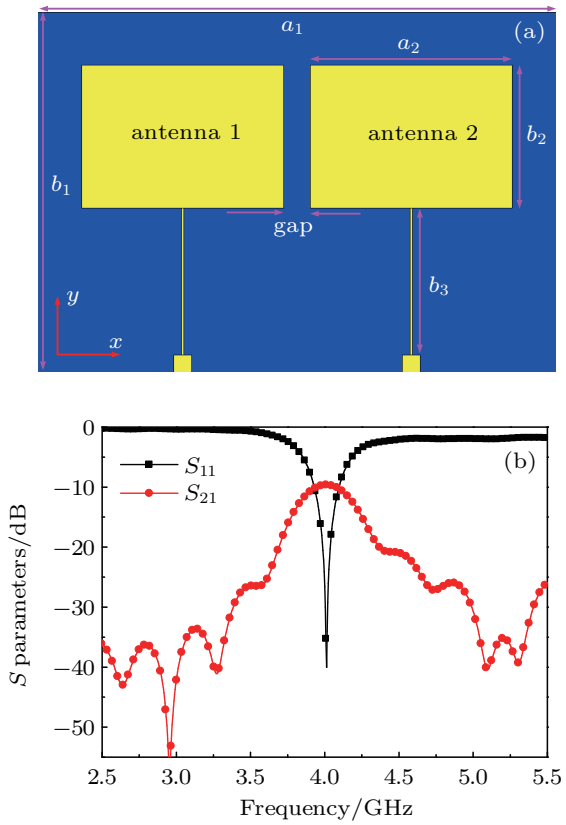



**Fig. 3.** (color online) Structure of the original proposed antenna array (a) and simulated result (b).

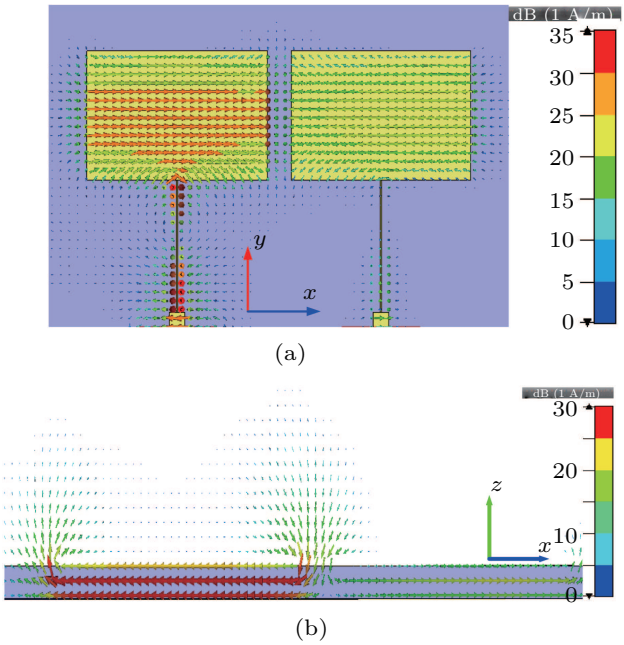



**Fig. 4.** (color online) *H*-field vector distribution of the two closely packed patches (a) on *xy* plane and (b) on *xz* plane in the substrate at 4 GHz.

### 2.3. Decoupling patch antennas using magnetic metamaterials

From the above analysis, to reduce the mutual coupling between adjacent patch antennas, it is crucial to suppress NFMC from the active antenna to adjacent antennas via the shared substrate. To this end, we integrate two SI-SRRs in between the two patches, as shown in Fig. 5(a). It should be noted that the center operation frequency of SI-SRRs has a minor shift since the boundary conditions are changed. To make sure that the operation frequency of the antennas falls into the negative permeability regime of SI-SRRs, we sweep $l_2$ with the other parameters unchanged. The optimized result is obtained when $l_2 = 5.25$ mm.

The simulated $S$ parameters of the antenna array with SI-SRRs are plotted in Fig. 5(b). It can be found that the center operation frequency has a very slight blue shift, from the original 4.0 GHz to 4.02 GHz. At the operating frequency, the magnitude of $S_{21}$ is about $-19.5$ dB, reduced by about 10 dB compared with the case without SI-SRRs. Figures 6(a) and 6(b) give the $H$-field vectors in the substrate at 4.02 GHz on $xy$ plane and $xz$ plane, respectively. From Fig. 6(a), we can see that the $H$-field vectors are restricted around the active antenna, while the NFMC into the passive antenna is held down effectively. Figure 6(b) shows that the $H$-field vectors penetrating into the adjacent passive antenna are suppressed by the SI-SRRs. This demonstrates that the NFMC in the substrate under the two patches is significantly suppressed.

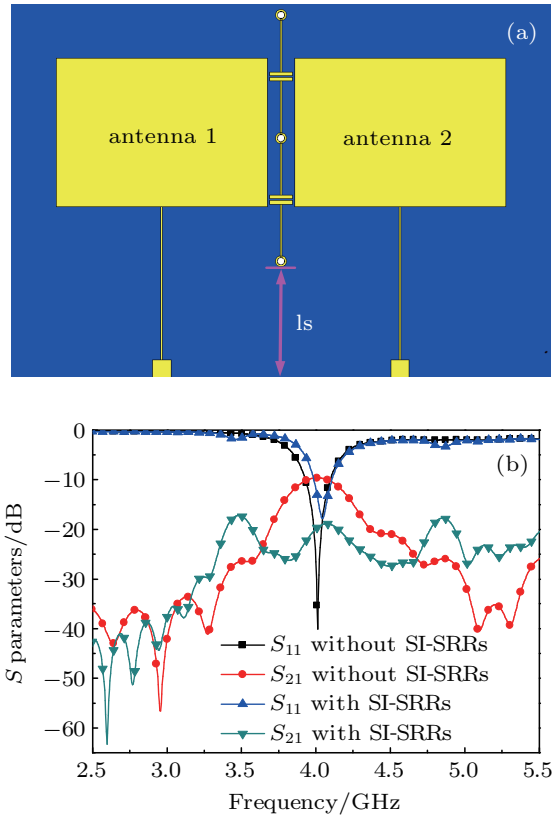



**Fig. 5.** (color online) Structure of the proposed antenna array with SI-SRRs (a) and simulated result (b).

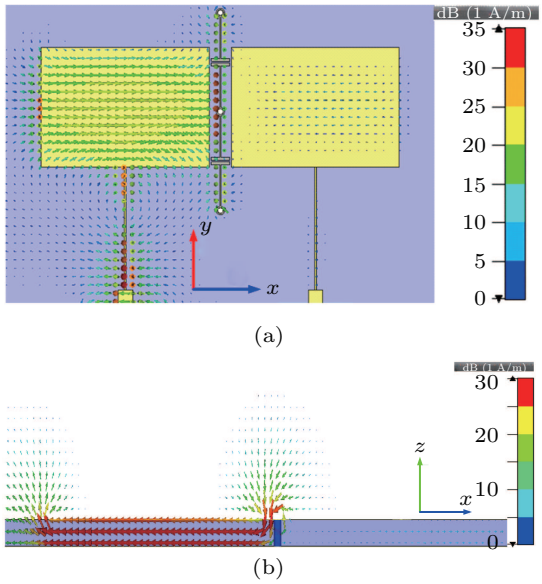



**Fig. 6.** (color online) $H$-field vectors on $xy$ plane (a) and $xz$ plane (b) in the substrate at 4.02 GHz.

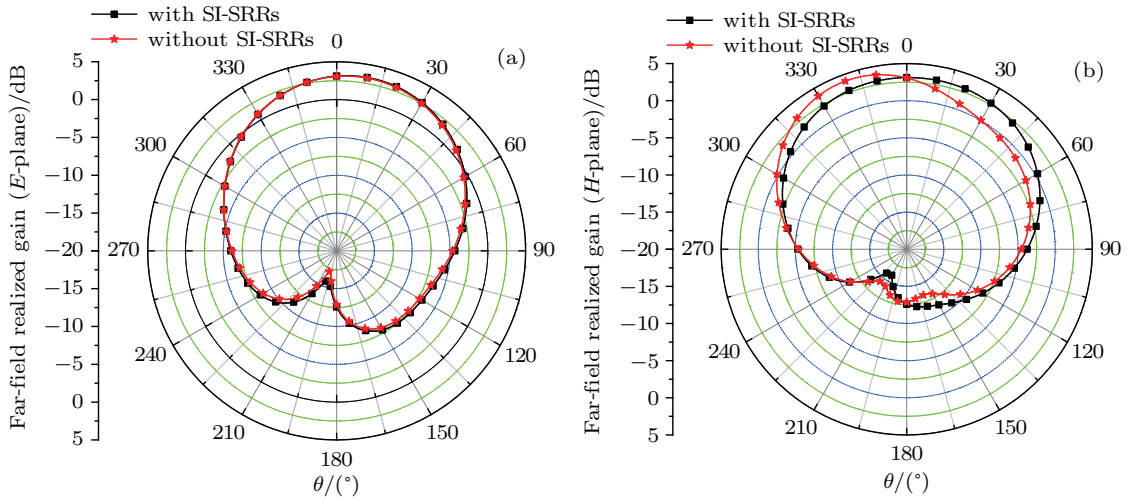



**Fig. 7.** (color online) Simulated far-field realized gain and radiation patterns of antennas with/without SI-SRRs at 4.0 GHz in (a) $E$-plane ($\phi = 90°$) and (b) $H$-plane ($\phi = 0°$) when antenna 1 is fed.

In order to check the effect of SI-SRRs on radiation patterns and the gain of antennas, the simulated far-field radiation patterns and realized gain for the antennas with and without SI-SRRs at 4.0 GHz on $E$-plane and $H$-plane are plotted in Figs. 7(a) and 7(b), respectively. From Fig. 7(a), we can find that the $E$-planes of antennas with and without IS-SRRs are almost the same. In this plane, far-field realized gain in main lobe is 3.53 dB. The main lobe direction and 3-dB angular width is 10° and 89.5°, respectively. In $H$-plane, the far-field realized gain in main lobe of antennas with and without IS-SRRs are 4.51 dB and 3.22 dB, respectively. The gain of antennas with SI-SRRs is reduced by 1.29 dB compared to that without SI-SRRs. However, the 3-dB angular width of antennas with SI-SRRs is 141.5°, about twice times that without SI-SRRs (the 3-dB angular width is of 71.7°). The main lobe direction is changed from −20° to 3° with the SI-SRRs.

## 3. Experimental verification

For further verification, two antenna arrays, one without and the other with SI-SRRs, were fabricated and measured. The fabricated prototypes and the measured results are all given in Fig. 8. $S$ parameters of the prototype antenna and the reference antenna were measured in the continuous band of 2.5 GHz–5.5 GHz in the microwave anechoic chamber. The measured results are given in Figs. 8(b) and 8(d). As shown in the measured results, at the operating frequency of the antennas, there is a very slight blue-shift for the operating frequencies of both the patch antenna arrays with and without SI-SRRs. The slight shift in both cases is due to smaller permittivity of the practically-used dielectric substrate. As shown in Figs. 8(b) and 8(d), the measured $S_{11}$ parameters at the operating frequency in the two cases are all below −20 dB, indicating a good impedance matching in the feeding port. The measured $S_{21}$ parameter is about −8.6 dB for the reference antennas while the measured $S_{21}$ parameter is drastically reduced down to −25.7 dB for the antennas loaded with SI-SRRs. Therefore, the mutual coupling is reduced by about 17.1 dB, indicating that the NFMC in the shared substrate has been significantly suppressed. This convincingly verifies the decoupling technique of patch antenna array is reliable and effectual.

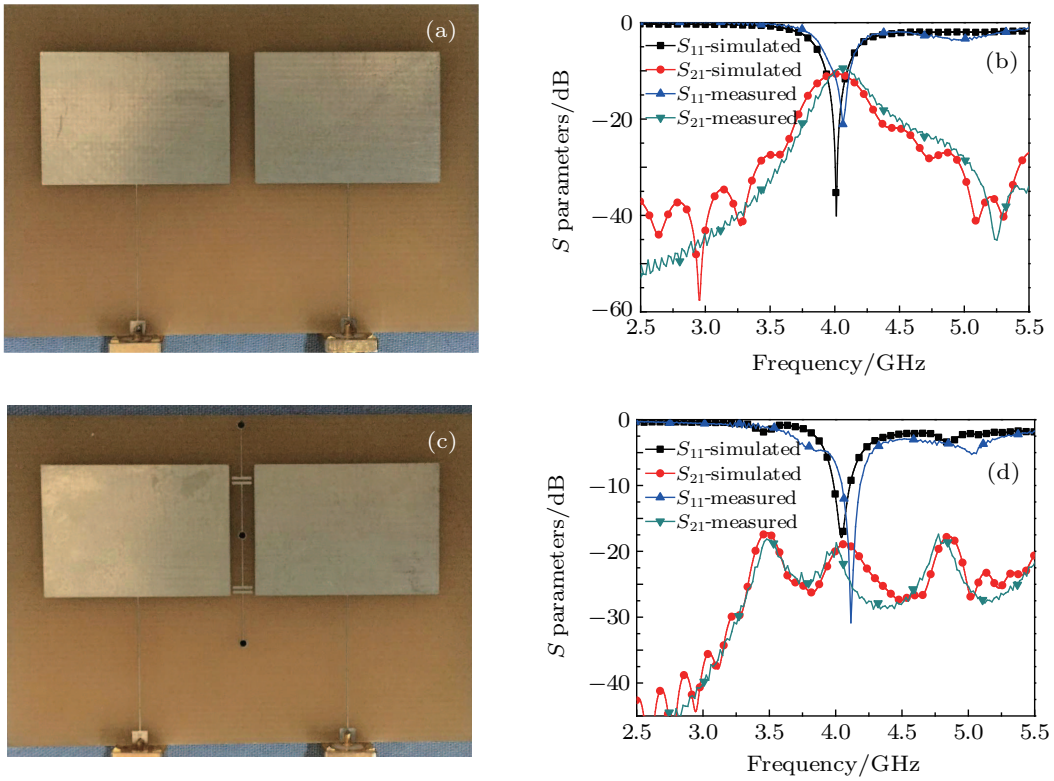



**Fig. 8.** (color online) (a) Fabricated prototype of the reference antennas. (b) Measured $S$ parameters of the reference antennas. (c) Fabricated prototype of the antennas with SI-SRRs. (d) Measured $S$ parameters of antennas with SI-SRRs.

Figure 9 presents the measured radiation patterns of antennas without and with SI-SRRs in $E$-plane and $H$-planes when antenna 1 is fed at 4.0 GHz. The simulated and measured $E$-planes of antennas with and without SI-SRRs are plotted in Figs. 9(a) and 9(b), respectively. Figures 9(c) and 9(d) show the simulated and measured $H$-plane radiation patterns with and without SI-SRRs. From Fig. 9, we observe that the measured radiation patterns are in accord with simulated ones. This verifies that the decoupling technique can lead to a broader beam-width on $H$-plane, which is favorable for phased array antennas.

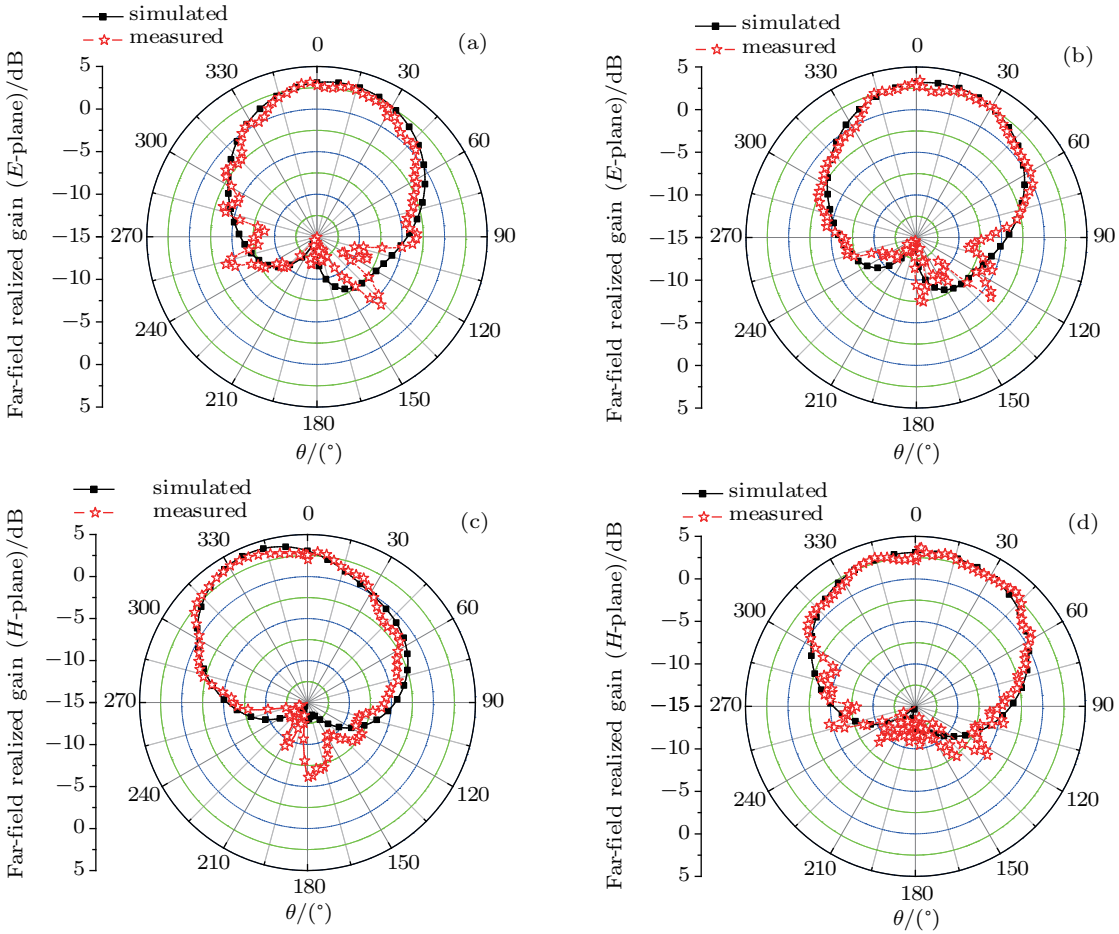



**Fig. 9.** (color online) Measured radiation patterns of antennas without SI-SRRs in (a) $E$-plane ($\phi = 90°$) and (c) $H$-plane ($\phi = 0°$), and antennas with SI-SRRs in (b) $E$-plane ($\phi = 90°$) and (d) $H$-plane ($\phi = 0°$) when antenna 1 is fed at 4.0 GHz.

## 4. Conclusion

In summary, we have demonstrated the decoupling technique of patch antenna array by suppressing NFMC using magnetic metamaterials. To deal with the strong NFMC in-substrate between adjacent antennas, we propose to use negative permeability of substrate-integrated magnetic metamaterials to block the magnetic fields. Since the magnetic metamaterials is highly integrated in substrate, this technique needs no additional space at all. To verify the technique, a prototype, together with a reference antenna array, was fabricated and measured. The measured results show that the isolation of the antenna array is increased by 17.1 dB when the gap between the two patch antennas is about $0.067\lambda$. This decoupling technique provides an effective alternative to high-isolation antenna array.

## References


[1] Foschini G J 1996 *Bell Labs Tech. J.* **1** 4159

[2] Wallace J W and Jensen M A 2003 *IEEE Trans. Wire. Commun.* **2** 335343

[3] Debatosh Guha 2011 *Microstrip and Printed Antennas: new trends, techniques, and applications* (New York: John Wiley & Sons)

[4] Lu Y F and Lin Y C 2013 *IEEE Microw. Anten. Propag.* **7** 754759

[5] Yang L, Fan M, Chen F, She J and Feng Z 2005 *IEEE Trans. Microw. Theory Tech.* **53** 183190

[6] Lai X Z and Xie Z M 2013 *IEEE Antennas Wirelss. Propag. Lett.* **12** 16301633

[7] Mohammad S Sharawil and Ahmed B Numanl 2013 *Prog. Electrom. Res.* **134** 247266

[8] Chiu C Y, Member, Cheng C H and Murch R D 2007 *IEEE Trans. Anten. Propag.* **55** 1735

[9] Xu H X and Wang G M 2013 *IEEE Trans. Magn.* **49** 1526

[10] Wu B I, Chen H S and Kong J A 2007 *J. Appl. Phys.* **101** 114913

[11] Dadashzadeh G and Dadgarpour A 2011 *IEEE Microw. Anten. Propag.* **5** 113125

[12] Pendry J B, Holden A J, Robbins D J and Stewart W J 1999 *IEEE Trans. Microw. Tech.* **47** 2075

[13] Wang J F and Qu S B 2010 *Phys. Rev. Lett.* **81** 036601

[14] Wang J S and Qu S B 2008 *IEEE Trans. Anten. Propag.* **56** 20182022

[15] Atsushi Ishikawa and Takuo Tanaka 2006 *Opt. Commun.* **258** 300305

[16] Bhattacharyya A K and Garg R 1985 *IEE Proc. pt. H* **132** 9398

[17] Lo Y T, Solomon D and Richards W F 1979 *IEEE Trans. Anten. Propag.* **27** 137145